© 2015. Published by The Company of Biologists Ltd | Journal of Cell Science (2015) 128, 768–780 doi:10.1242/jcs.162362

RESEARCH ARTICLE

Presynaptic NMDA receptors – dynamics and distribution in developing axons *in vitro* and *in vivo*

Ishwar Gill[1,*], Sammy Droubi[1,*], Silvia Giovedi[2,*], Karlie N. Fedder[1], Luke A. D. Bury[1], Federica Bosco[2], Michael P. Sceniak[3], Fabio Benfenati[2,4] and Shasta L. Sabo[1,3,‡]

ABSTRACT

During cortical development, N-methyl-D-aspartate (NMDA) receptors (NMDARs) facilitate presynaptic terminal formation, enhance neurotransmitter release and are required in presynaptic neurons for spike-timing-dependent long-term depression (tLTD). However, the extent to which NMDARs are found within cortical presynaptic terminals has remained controversial, and the sub-synaptic localization and dynamics of axonal NMDARs are unknown. Here, using live confocal imaging and biochemical purification of presynaptic membranes, we provide strong evidence that NMDARs localize to presynaptic terminals *in vitro* and *in vivo* in a developmentally regulated manner. The NR1 and NR2B subunits (also known as GRIN1 and GRIN2B, respectively) were found within the active zone membrane, where they could respond to synaptic glutamate release. Surprisingly, NR1 also appeared in glutamatergic and GABAergic synaptic vesicles. During synaptogenesis, NR1 was mobile throughout axons – including growth cones and filopodia, structures that are involved in synaptogenesis. Upon synaptogenic contact, NMDA receptors were quickly recruited to terminals by neuroligin-1 signaling. Unlike dendrites, the trafficking and distribution of axonal NR1 were insensitive to activity changes, including NMDA exposure, local glutamate uncaging or action potential blockade. These results support the idea that presynaptic NMDARs play an early role in presynaptic development.

KEY WORDS: NMDA receptor, Receptor trafficking, Synapse development, Synaptosome, Presynaptic

INTRODUCTION

Presynaptic N-methyl-D-aspartate (NMDA) receptors (NMDARs) have been suggested to play roles in cortical synapse development (Corlew et al., 2007). They have also been linked to pathogenesis of developmental disorders, including epilepsy (Yang et al., 2007; Yang et al., 2006) and fetal alcohol spectrum disorders (Valenzuela et al., 2008). However, the existence of presynaptically localized NMDARs at cortical synapses has remained controversial for decades.

During cortical development, activation of NMDARs in presynaptic neurons facilitates neurotransmitter release and is required for spike-timing-dependent long-term depression (tLTD) (Berretta and Jones, 1996; Brasier and Feldman, 2008; Buchanan et al., 2012; Corlew et al., 2007; Rodríguez-Moreno and Paulsen, 2008; Sjöström et al., 2003). Although dendritic NMDARs might contribute to presynaptic plasticity (Christie and Jahr, 2008; Christie and Jahr, 2009), axonal NMDARs are necessary for tLTD (Rodríguez-Moreno et al., 2011). In addition, Ca^{2+} transients are observed in presynaptic boutons upon focal uncaging of NMDA or glutamate (Buchanan et al., 2012; McGuinness et al., 2010). However, it is not clear whether the responsible axonal receptors are distributed throughout the axon or whether they are enriched at nerve terminals (Buchanan et al., 2012). If they localize to presynaptic terminals, it is unknown which presynaptic structures contain NMDARs. Understanding where axonal NMDARs are located is important because axonal NMDARs might (1) utilize distinct signaling mechanisms, (2) be activated by different sources and levels of glutamate (e.g. synapse-autonomous glutamate release versus spill-over or ambient glutamate, or spontaneous versus evoked release), or (3) serve distinct functions (e.g. control of plasticity at the level of individual synapses, axon branches or entire arbors) based on where they reside.

NMDARs in presynaptic neurons regulate neurotransmitter release before onset of the critical period for receptive field plasticity (Corlew et al., 2007). Furthermore, axonal NMDAR expression is highest during the postnatal first two weeks, a period of intense synapse formation, but is dramatically decreased later in development (Corlew et al., 2007; Ehlers et al., 1998; Herkert et al., 1998; Song et al., 2009; Wang et al., 2011). Therefore, it has been hypothesized that presynaptic NMDARs might facilitate synapse formation (Corlew et al., 2008). If so, it would be expected that NMDARs are expressed at nascent presynaptic terminals, but it is not known whether this is the case. In addition, the specific functions of presynaptic NMDARs is defined by when and where they are present: NMDARs can participate in early steps in synaptogenesis only if they are present during those steps, whereas late arrival to presynaptic terminals would support a role in presynaptic maturation or plasticity but not initial synaptogenesis.

To address these issues, we defined the spatio-temporal dynamics of axonal NMDARs during cortical synapse formation using a combination of live time-lapse confocal microscopy of NMDAR subunits, immuno-isolation of synaptic vesicles and ultrasynaptic fractionation of presynaptic terminals. NR1 (also known as GRIN1) appeared in discrete puncta throughout the axons of many cortical neurons during periods of intense synapse formation. Some NR1 puncta were mobile, whereas others

[1]Department of Pharmacology, Case Western Reserve University School of Medicine, Cleveland, OH, 44106, USA. [2]Department of Experimental Medicine, University of Genoa, 16132 Genoa, Italy. [3]Department of Neuroscience, Case Western Reserve University School of Medicine, Cleveland, OH, 44106, USA. [4]Department of Neuroscience and Brain Technologies, Istituto Italiano di Tecnologia, 16163 Genoa, Italy.
*These authors contributed equally to the study

‡Author for correspondence (shasta.sabo@case.edu)

Received 27 August 2014; Accepted 5 December 2014

Journal of Cell Science

Journal of Cell Science (2015) 128, 768–780 doi:10.1242/jcs.162362

localized to presynaptic terminals. NMDARs were recruited to terminals within 24 h, and contact with neuroligin-expressing cells was sufficient to induce this recruitment. The distribution and trafficking of axonal NMDARs was insensitive to acute changes in activity. Within presynaptic terminals *in vivo*, NR1 associated with the presynaptic active zone membrane and, surprisingly, both glutamatergic and GABAergic synaptic vesicles. These data provide strong evidence that NMDARs are integral to developing presynaptic terminals and are in the right place at the right time to locally regulate early steps in presynaptic development.

RESULTS

NMDARs are present in axons and presynaptic terminals of developing neocortical neurons

Because the existence and localization of presynaptic NMDARs in cortical neurons has been controversial, we first determined where NMDARs are found in the axons of developing neocortical neurons. To do so, we transfected cultured visual cortical neurons at 5–6 days *in vitro* (DIV) with GFP-tagged rat NR1 isoform 1a. NR1 is an obligate subunit of functional NMDARs (Granger et al., 2011). Previous studies have shown that transfecting neurons with NR1 does not lead to the overexpression of NR1 or increase the number of functional NMDARs, and that GFP-tagged NR1 accurately reflects the localization of endogenous NR1 in dendrites (Bresler et al., 2004; Luo et al., 2002; Prybylowski et al., 2002; Washbourne et al., 2002). Similarly, there was no increase in NR1 immunofluorescence in dendrites of our neurons when transfected with NR1–GFP as compared to neighboring neurons within the same culture that were not transfected (mean intensity for transfected, 80.2% of control untransfected; standard deviation of intensity, 117.5% of untransfected; maximum intensity, 92.5% of untransfected). To identify axons, neurons were co-transfected with synaptophysin–mRFP (or synaptophysin–mCherry). Transfected axons were initially identified based on a combination of criteria: (1) expression of synaptophysin–mRFP in a punctate pattern typical of axons, (2) non-tapering morphology, and (3) length of the processes, because axons typically extend farther than dendrites at this stage of development. Axons were then imaged live to determine the presence of NR1–GFP. Axonal identity was ultimately confirmed through retrospective double-immunofluorescence with antibodies against MAP2 and tau-1: MAP2 is highly enriched in dendrites and nearly absent from axons, whereas tau-1 is typically enriched in axons (Bernhardt and Matus, 1984; Binder et al., 1985; Kosik and Finch, 1987). Given that the absence of MAP2 was more reliable than the enrichment in tau for identifying axons in our developing cortical neurons, most of the experiments described below used the absence of MAP2 to identify axons.

Live confocal imaging of NR1–GFP indicated that many axons expressed NR1–GFP in discrete puncta (Fig. 1A,B). Axonal NR1–GFP puncta typically appeared smaller, dimmer and less dense than dendritic NR1–GFP in the same neuron (Fig. 1C). Axonal NR1 puncta appeared at a mean density of 0.04 puncta/μm and as high as 0.06 puncta/μm. In addition, some axons had spots of NR1 enrichment that appeared brighter than the background in the rest of the axon, but were less bright and more diffuse than typical NR1 puncta and were consequently below the minimum threshold intensity for puncta detection. The density of enriched-spots plus puncta was 0.1/μm.

Endogenous NR1 also was found in puncta in axons (Fig. 1D). In order to clearly distinguish axonal NR1 from NMDARs in dendrites and glia, endogenous NR1 was examined in neurons grown without contact with glia and regions of axon that did not contact dendrites. Therefore, the punctate distribution of NR1 does not depend on contact with dendrites or glia. NR1 puncta might correspond to clusters of NR1 in the axonal plasma membrane, vesicles transporting NR1 along axons, or both.

To determine the extent to which NR1 is found at presynaptic terminals, we examined NR1–GFP and synaptophysin–mRFP in the same axons (Fig. 1B; Fig. 2A). NR1 and synaptophysin puncta

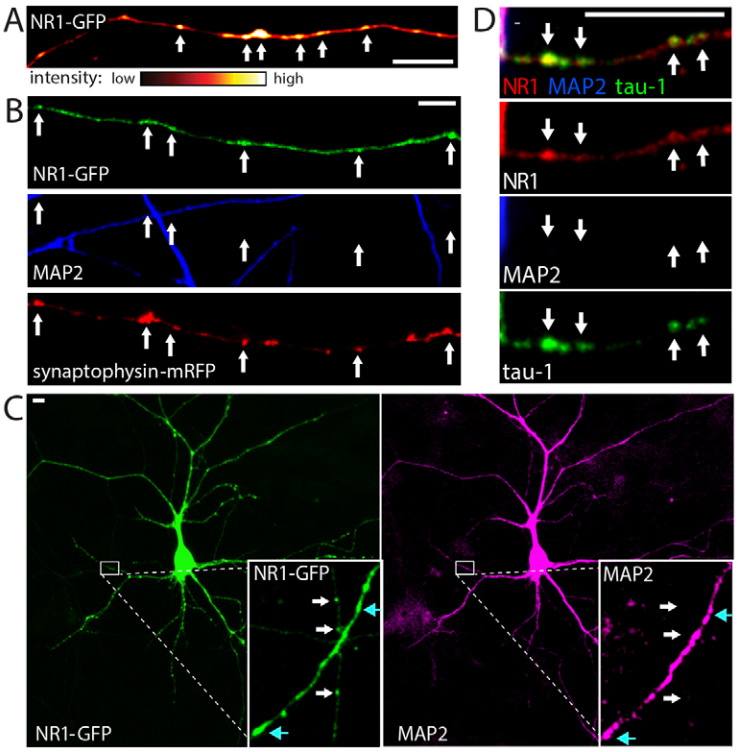

Fig. 1. NR1 is found in puncta along axons of developing neocortical neurons. Neurons were co-transfected with NR1–GFP and synaptophysin–mRFP. Axons were identified independently of the NR1 signal by using synaptophysin–mRFP fluorescence, and axonal identity was confirmed by the specific lack of MAP2 staining in retrospective immunofluorescence. (A) The NR1 signal is punctate in many axons. NR1 fluorescence is pseudocolored according to the indicated scale. (B) Images showing NR1 puncta (green, top panel) in an axon that is MAP2-negative axon (blue, middle panel) but synaptophysin-positive (red, bottom panel). Locations of individual NR1 puncta are indicated by arrows in each panel. (C) Low magnification images of a neuron expressing NR1–GFP (green, left) and immunolabeled for MAP2 (magenta, right). The region within the white box is shown at higher magnification (inset). NR1 puncta in the MAP2-negative axon are indicated by white arrows, whereas dendritic NR1 puncta are indicated by cyan arrows. Axonal NR1 puncta are typically smaller and less bright than dendritic NR1 in the same neuron (the NR1–GFP signal is saturated in the soma to allow visualization of axonal NR1). (D) Immunofluorescence images showing the localization of endogenous NR1 within an axon. Axons were located using tau (green, bottom panel) and their identity confirmed by the absence of MAP2 immunoreactivity (blue, third panel). NR1 (red, second panel) is found in puncta along axons (arrows). The top panel shows the overlay of all three channels. Scale bars: 10 μm.

Journal of Cell Science (2015) 128, 768–780 doi:10.1242/jcs.162362

were identified in each channel independently, based on image statistics (Fig. 2B). Synaptophysin colocalized with 50.2±10.3% of NR1 puncta (mean±s.e.m.; $n=77$). Conversely, NR1 colocalized with 51.1±8.2% of synaptophysin puncta ($n=78$). Of the colocalized puncta, 91.9% of NR1 puncta overlapped with synaptophysin and 8.1% were adjacent to synaptophysin. Endogenous NR1 also colocalized with synaptophysin within axons (Fig. 2C).

We then determined whether the NR1 and synaptophysin signals were correlated. Cross-covariograms were made for NR1 and synaptophysin signals in each transfected axon, and the peaks of the cross-covariograms, which correspond to the degree of correlation between the two signals, were quantified (Fig. 2D). The degree of correlation varied (range, 0.1079–0.7651; mean, 0.4786; $n=11$ axons), with a significant correlation occurring in 54.6% of axons (peak of covariogram>0.5, centered at 0 displacement). This indicates that in a population of axons, NR1 and synaptophysin signals are not only colocalized but also that their intensities co-vary.

To verify that sites of NR1 and synaptophysin colocalization correspond to presynaptic terminals, we imaged axo-dendritic contacts formed between (1) axons that expressed NR1–GFP and synaptophysin–mRFP, and (2) MAP2-labeled dendrites and somas of neurons that were not transfected (Fig. 2E). This ensured that the observed NR1 was restricted to the axon. At least one NR1 punctum was found in 84.9±6.5% of axo-dendritic contacts ($n=63$ contacts from 20 images). NR1-positive axo-dendritic contact sites also contained synaptophysin. These data strongly support the hypothesis that NR1 is found at presynaptic terminals of cortical neurons.

NMDARs are integral to the presynaptic active zone and synaptic vesicles of developing glutamatergic and GABAergic synapses

Next, we verified that NMDARs localize to presynaptic terminals and determined where they reside within presynaptic terminals by using ultrastructural fractionation of synaptosomes (Fig. 3A), as previously described (Feligioni et al., 2006; Phillips et al., 2001; Pinheiro et al., 2005; Pinheiro et al., 2003). First, we verified the purity of the fractionation by immunoblotting for synaptophysin and the postsynaptic proteins PSD95 (also known as DLG4) and SHANKs (Fig. 3B). The majority of synaptophysin appeared in the non-synaptic synaptosomal protein (NSSP) fraction, which contains all synaptic cytosolic and membrane proteins that are not directly incorporated in or strongly associated with the active zone or postsynaptic density, including most synaptic vesicles. The small amount of synaptophysin in the active zone fraction is thought to correspond to docked synaptic vesicles (Feligioni et al., 2006). By contrast, PSD95 and SHANK proteins were exclusively found in the postsynaptic density (PSD) fraction. PSD95 and SHANK proteins were absent from the active zone (AZ) and NSSP fractions, regardless of the exposure times.

As expected, NR1 was abundant in the PSD fraction of both developing (P12) and adult synapses. However, in contrast to PSD95, NR1 was also observed in the AZ fraction and, to a lesser extent, in the NSSP fraction in developing synapses (Fig. 3B). Although a small amount of NR1 appeared in the AZ fraction in adults, the levels in adult appeared to be substantially reduced when compared to developing synapses. Similar to NR1, NR2B (also known as GRIN2B) was also observed in the AZ fraction of developing synapses, but NR2B was absent from the AZ fraction of mature synapses, even at long exposures. During development, synaptic NR2 subunits undergo a switch from predominantly

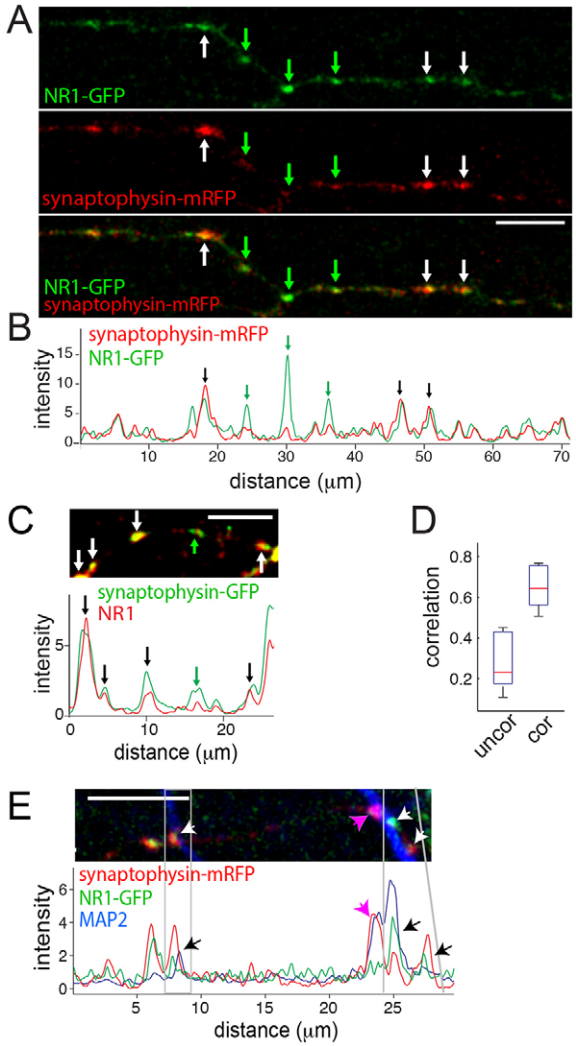

Fig. 2. NR1 and synaptophysin puncta colocalize at presynaptic terminals. (A) Images of NR1–GFP and synaptophysin–mRFP in the same axon. Many NR1 puncta colocalize with synaptophysin, whereas others do not. (B) Line-intensity plot illustrating that NR1 and synaptophysin puncta often colocalize within axons. The green and red lines represent the intensity of NR1–GFP and synaptophysin-mRFP fluorescence along the axon, respectively. In A and B, white and black arrows indicate puncta with both NR1 and synaptophysin, whereas green arrows indicate locations of puncta with only NR1. (C) Images (top) and line-intensity plot (bottom) showing that endogenous NR1 (red) colocalizes with synaptophysin–GFP puncta (green) within axons. Neurons were transfected with synaptophysin–GFP then immunolabeled for NR1. Colocalization is indicated by white and black arrows. (D) Box plots showing a quantification of the degree of correlation (peak covariance) between NR1 and synaptophysin in all axons with (cor) and without (uncor) a significant correlation. The box represents the 25–75th percentiles, and red line indicates the median. The whiskers extend to the most extreme data points, not considered outliers, and correspond to approximately ±2.7σ. $n=11$ axons. (E) Top, fluorescence image showing NR1 (green) and synaptophysin (red) localization at axo-dendritic contacts (white arrows; dendrites are indicated by MAP2 in blue). Bottom, line-intensity plot of relative intensity of MAP2 (blue), NR1–GFP (green), and synaptophysin–RFP (red) for the image shown, with colocalization occurring at three distinct sites of axo-dendritic contact (black arrows). The pink arrows indicate a presynaptic terminal in the same axon that lacks NR1. Scale bars: 10 μm.

NR2B-containing to NR2A-containing receptors. Here, NR2A levels were higher in PSDs of adults when compared to developing synapses, and NR2A was absent from the active zone fraction at both ages, even at the longest exposures possible.

Journal of Cell Science (2015) 128, 768–780 doi:10.1242/jcs.162362

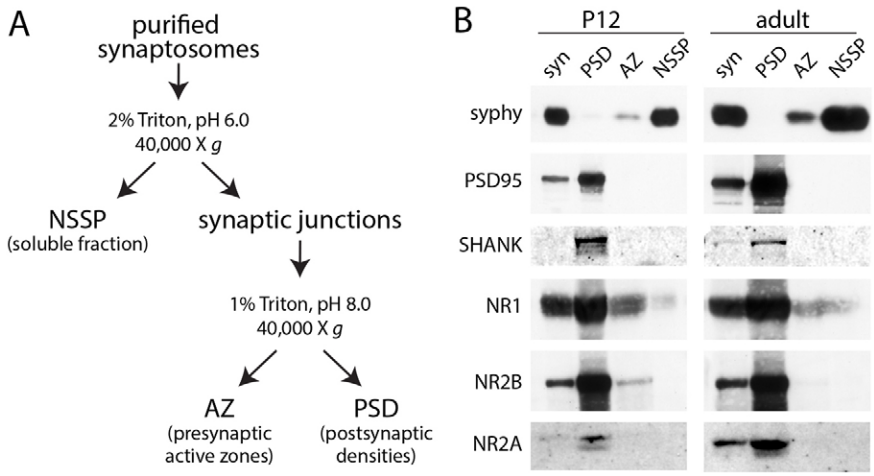

Fig. 3. NR1 resides in the active zones of developing presynaptic terminals. (A) Schematic of the ultrasynaptic purification of purified synaptosomes. (B) Ultrasynaptic distribution of NMDA receptor subunits in purified synaptosomal fractions. Synaptosomes from P12 and adult mouse brain were subjected to ultrasynaptic fractionation to separate the postsynaptic density (PSD), presynaptic active zone region (AZ) and solubilized non-synaptic synaptosomal protein (NSSP) compartments (Feligioni et al., 2006). Aliquots of total synaptosomes (syn) and of each ultrasynaptic fraction (10–30 μg) were probed with antibodies against NR1, NR2B and NR2A, and against marker proteins [synaptophysin (syphy), PSD95 and SHANK proteins] to validate ultrasynaptic compartments.

Taken together, these data indicate that NR2B-containing NMDARs are an integral component of the active zones of developing synapses and that association of NMDARs with the active zone is developmentally regulated.

Previous work has shown that α-amino-3-hydroxy-5-methyl-4-isoxazolepropionic acid (AMPA) receptors (AMPARs) are found in small synaptic vesicles (Schenk et al., 2003); therefore, we next asked whether NMDARs associate with synaptic vesicles. To test this hypothesis, synaptic vesicles were immunoisolated from lysed synaptosomes using antibodies against glutamate and γ-aminobutyric acid (GABA) vesicular transporters. Remarkably, NR1 was associated with VGLUT1-, VGLUT2- and VGAT-positive synaptic vesicles from P6 brains (Fig. 4A,C,D), indicating that NMDARs are present in both excitatory and inhibitory presynaptic terminals during postnatal development (P6). This localization was developmentally regulated because NR1 was not observed in synaptic vesicles from adult brain (Fig. 4B–D), as previously reported (Schenk et al., 2003). The appearance of NR1 in both excitatory and inhibitory synaptic vesicles was specific because VGAT did not co-immunoisolate with VGLUTs and vice versa (Fig. 4E,F). Importantly, PSD95 was not observed in the synaptic vesicle immunoisolates or even in the starting material for the immunoisolation, the LS1 fraction (Fig. 4G). In addition, traces of NR1 were also evident in synaptic vesicles purified by ultra-pure controlled-pore glass chromatography (Fig. 4G). This synaptic vesicle location suggests that presynaptic NMDARs can be taken up from the presynaptic membrane by endocytosis and/or delivered to the presynaptic membrane upon exocytosis.

NMDARs are transported along developing axons independently of STVs

We next asked how and when NMDARs are delivered to presynaptic terminals. To address this, NR1–GFP-expressing axons were subjected to live, time-lapse imaging (every 30 s for 25 frames). From this analysis, it was clear that a population of NR1 puncta was mobile (Fig. 5A–C; supplementary material Movie 1). NR1 puncta moved in 54.2% of axons (13 of 24). In these axons, 24.5±6.6% of puncta were mobile (mean±s.e.m.; n=139 puncta in 13 axons), moving anterogradely, retrogradely or both. Interestingly, in one axon, an NR1 punctum spontaneously formed from a more diffuse pool of NR1, suggesting that at least some NR1 puncta form from NR1 that is already in the axon (Fig. 5D).

The individual movements of 21 puncta were then tracked and quantified. The majority (67.7%) of puncta moved unidirectionally and at a fairly consistent velocity (Fig. 5A,B). A smaller subset of puncta (14.3%) displayed highly saltatory movement, sometimes pausing for several frames and/or switching direction (Fig. 5B). On average, mobile NR1 puncta spent half of their time moving (53.0±9.7%), with two distinct populations of puncta that moved either >80% or <35% of the time (Fig. 5C). NR1 puncta moved continuously for an average of 112.7±27.1 s (Fig. 5C; n=32 continuous movements). The instantaneous velocities of mobile NR1 puncta were variable, with a maximum velocity of 0.59 μm/s and a mean instantaneous velocity of 0.23±0.01 μm/s (Fig. 5C).

During synapse formation, many synaptic vesicle and several active zone proteins are prepackaged together into Golgi-derived transport organelles, known as synaptic vesicle protein transport vesicles (STVs), for delivery to developing presynaptic terminals. This raises the question of whether NMDARs are delivered to presynaptic terminals in STVs together with synaptic vesicle proteins. To test this, we asked whether NR1–GFP and synaptophysin–mRFP move together along axons (Fig. 5E). NR1 puncta and synaptophysin puncta could be observed moving together; however, the majority of mobile NR1 puncta movements were independent of synaptophysin puncta, with only 25.9±8.9% of NR1 puncta moving with synaptophysin at some point during imaging (n=53 NR1 puncta in seven axons; Fig. 5F). Similarly, the majority of mobile synaptophysin puncta moved independently of NR1, with only 30.7±8.0% of synaptophysin puncta moving with NR1 at some point (n=45 synaptophysin puncta; Fig. 5F). Of the puncta that exhibited co-movement of NR1 and synaptophysin, 41.7% showed only partial co-movement, and most consisted of only short movements of no more than 10 μm (Fig. 5F). In addition, the characteristics of NR1 movement were generally distinct from the typical characteristics of STVs: NR1 puncta tended to move for extended periods at a relatively consistent velocity and direction (Fig. 5A,B). In contrast, synaptophysin puncta typically have highly discontinuous movements, frequently pausing and reversing directions (Bury and Sabo, 2011; Sabo et al., 2006). Taken together, these data suggest that NR1 and most synaptic vesicle proteins are delivered independently to developing presynaptic terminals. It is worth noting that these data also argue against a significant contribution of transport intermediates to the colocalization observed above in Fig. 2,

Journal of Cell Science (2015) 128, 768–780 doi:10.1242/jcs.162362

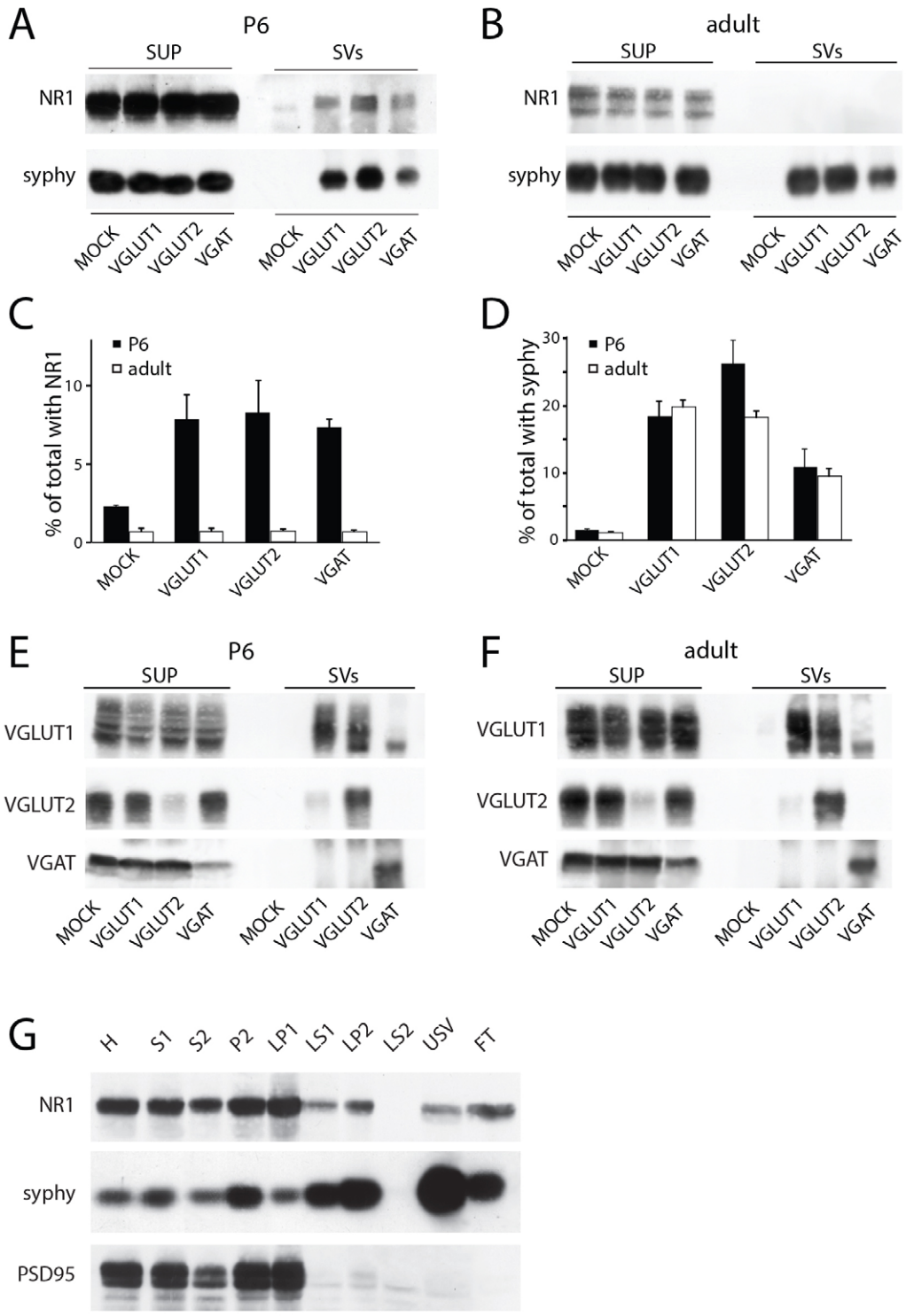

Fig. 4. See next page for legend.

further supporting the presynaptic identity of colocalized NR1 and synaptophysin.

The distribution and dynamics of axonal NMDARs are insensitive to neuronal activity

Within dendrites, NMDA receptor localization and trafficking can be acutely regulated by activity (Barria and Malinow, 2002; Grosshans et al., 2002; Heynen et al., 2000); therefore, we next asked whether axonal NR1 trafficking is regulated by activity (Fig. 6). Upon acute (10–15 min) treatment of neurons with NMDA (15–100 µM) to activate NMDARs, the density of NR1 puncta was unchanged (Fig. 6A; mean±s.e.m. percentage change in density 13.1±6.7, P=0.0667, repeated measures ANOVA). Similarly, exposure to TTX (1 µM) to inhibit action potential driven activity had no effect on NR1 density (mean percentage change in density, 9.0±9.2; P=0.4285). In addition, the

Fig. 4. NR1 appears in synaptic vesicles of developing glutamatergic and GABAergic presynaptic terminals. (A–D) Synaptic vesicles (SVs) were immunoisolated from lysed synaptosomes and subjected to immunoblotting for NR1 and synaptophysin (syphy). (A) NR1 is co-immunoisolated with synaptic vesicles from P6 mouse brain. NR1 appeared in glutamatergic vesicles isolated with either anti-VGLUT1 or -VGLUT2 antibodies, as well as in GABAergic vesicles isolated with anti-VGAT antibodies. SUP, supernatant after immunoisolation. SVs, synaptic vesicles immunoisolated using the antibodies indicated below each lane. Faint NR1 immunoreactive bands were visible upon mock immunoisolation with anti-rabbit-IgG antibodies (MOCK), but the intensity of these bands was always several fold lower than the bands observed in VGLUT and VGAT immunoisolates (see quantification in C). (B) NR1 is not associated with synaptic vesicles from adult brain. Quantification of the percentage of total NR1 (C) and synaptophysin (D) immunoreactivities (mean±s.e.m., $n=3$ experiments) associated with synaptic vesicles that were immunoisolated from P6 (black) and adult (white) forebrains with the indicated antibodies. (E,F) Immunoisolation of glutamatergic and GABAergic synaptic vesicles was specific. Glutamategic SVs were not immunoisolated with beads coupled with VGAT or with anti-rabbit IgGs (MOCK). Similarly, GABAergic synaptic vesicles were not immunoisolated using beads coupled with either rabbit VGLUT1, VGLUT2 or anti-rabbit IgGs. (G) Subcellular distribution of NMDARs. Subcellular fractions of young rat forebrain obtained at various stages of vesicle purification were analyzed by immunoblotting for NR1, synaptophysin and PSD95. NR1 is present in the LS1 fraction and is further enriched in LP2, traces are also evident in highly purified synaptic vesicles. H, homogenate; S1, postnuclear supernatant; S2, supernatant of P2; P2, crude synaptosomes; LP1, crude synaptic plasma membranes after osmotic lysis; LS1, supernatant of LP1; LP2, crude synaptic vesicles; LS2, synaptosol; USV, highly purified synaptic vesicles; FT, flow through. As expected, PSD95 is absent from LS1 and fractions derived from LS1, indicating that synaptic vesicle preparations (both here and in synaptic vesicle immunoisolations) are not contaminated with postsynaptic proteins.

percentage of mobile NR1 puncta was unchanged by either NMDA or TTX (Fig. 6B; NMDA mean percentage change 44.2±25.1, $P=0.2706$, $n=18$ axons; TTX, mean percentage change, 46.9±31.8, $P=0.4425$, $n=12$ axons; repeated measures ANOVA). The appearance and movements of NR1–GFP puncta were also unaffected by uncaging of glutamate near transfected axons (Fig. 6C; $P=0.218$ by repeated measures ANOVA, $n=5$ axons). Glutamate uncaging was effective at activating NMDARs because focal uncaging near dendrites induced formation of new dendritic spines (data not shown).

Neuroligin adhesion recruits NR1 to nascent presynaptic terminals

NMDARs regulate presynaptic development (Sceniak et al., 2012), but it is not known whether presynaptic NMDARs are in the right place at the right time to mediate NMDAR-dependent presynaptic development. If presynaptic NMDARs are involved in synaptogenesis, they would be expected to (1) arrive at nascent synapses fairly early and (2) assemble at presynaptic terminals in response to synaptogenic signals. One well-characterized synaptogenic signal is trans-synaptic adhesion mediated through neuroligin. Neuroligin adhesion induces formation of fully functional presynaptic terminals (Scheiffele et al., 2000), and synaptic vesicle and active zone proteins are stably recruited to these new boutons within the first day after contact (Bury and Sabo, 2014; Lee et al., 2010). In addition, NMDAR activation regulates development of presynaptic terminals that are induced by neuroligin adhesion (Sceniak et al., 2012).

Therefore, we determined whether neuroligin adhesion recruits NMDARs to sites of new presynaptic terminal assembly. To do so, HEK-293 cells were transfected with neuroligin-1 then placed in contact with NR1–GFP-transfected axons to induce *de novo* presynaptic terminal formation in the absence of dendrites. Within 24 h after contact was induced, NR1 appeared in discrete puncta at sites of adhesion with neuroligin-expressing HEK-293 cells (Fig. 7A,B). The average percentage of axon length covered by NR1 puncta was 17.3±3.4% (mean±s.e.m.) (Fig. 7C). This was significantly higher than the average percentage of axon length covered by NR1 puncta at non-contact regions of the axon (8.4±1.7%; $P=0.0273$, $n=12$ contacts). In addition, the average density of NR1 puncta at neuroligin contacts was approximately double that at non-contact regions of the axon (Fig. 7D; $P=0.0346$). When imaged live, NR1 was recruited to neuroligin contacts, even when other NR1 puncta were mobile within the same axon (Fig. 7E). These data indicate that synaptogenic adhesion is sufficient to induce stable recruitment of NR1 to nascent presynaptic terminals as they form. Interestingly, some NR1 passed by contact sites without being recruited, suggesting that there is a population of mobile NR1 that is unresponsive to the neuroligin–neurexin synaptogenic cue.

Dynamic NMDARs are present within structures that are involved in axonal synaptogenesis

NMDARs are present in axonal growth cones of immature hippocampal neurons (Ehlers et al., 1998; Herkert et al., 1998; Wang et al., 2011), but their dynamics within growth cones have not yet been reported. Consistent with these reports, we observed bright NR1–GFP puncta in axonal growth cones of developing cortical neurons. NR1 puncta were present in extending ($n=7$), retracting ($n=4$) and stationary ($n=6$) growth cones (Fig. 8; supplementary material Movie 2). NR1 fluorescence also appeared bright in nascent growth cones formed from existing axons, even as they emerged from the axon ($n=7$). Interestingly, in 71.4% of examples, NR1 clearly appeared at the site of growth cone initiation prior to emergence of a distinct growth cone.

Synaptic vesicle proteins can enter and leave growth cone filopodia and lamellopodia (Sabo and McAllister, 2003), raising the question of whether NMDARs are also dynamic within these regions of axonal growth cones. We found that NR1 fluorescence was often very bright in the central domain of the growth cone and in the region of the axon immediately proximal to the growth cone (Fig. 8). NR1 puncta was highly dynamic in both the growth cone and adjacent axon. NR1 puncta also appeared and disappeared from growth cone filopodia from one frame to the next. Of the imaged growth cones, 80.0% ($n=15$) had NR1 puncta that were transiently present in lamellipodia or filopodia. Interestingly, NR1 puncta also rapidly entered and exited axonal shaft filopodia (supplementary material Movie 2). Therefore, presynaptic NMDARs are in a position to contribute to synaptogenesis even during or before initial axo-dendritic contact.

DISCUSSION

NMDARs play key roles in cortical development, and it is likely that presynaptic NMDARs are responsible for some of these effects. For example, it has been suggested that presynaptic NMDARs could contribute to establishment of receptive field properties in the visual system, such as retinotopy, ocular dominance and orientation selectivity (Corlew et al., 2007). It has also been suggested that presynaptic NMDARs mediate some acute effects of brain-derived neurotrophic factor (BDNF), a strong regulator of cortical development (Madara and Levine, 2008). To understand when, where and how axonal and presynaptic NMDARs contribute to cortical development, it is

Journal of Cell Science (2015) 128, 768–780 doi:10.1242/jcs.162362

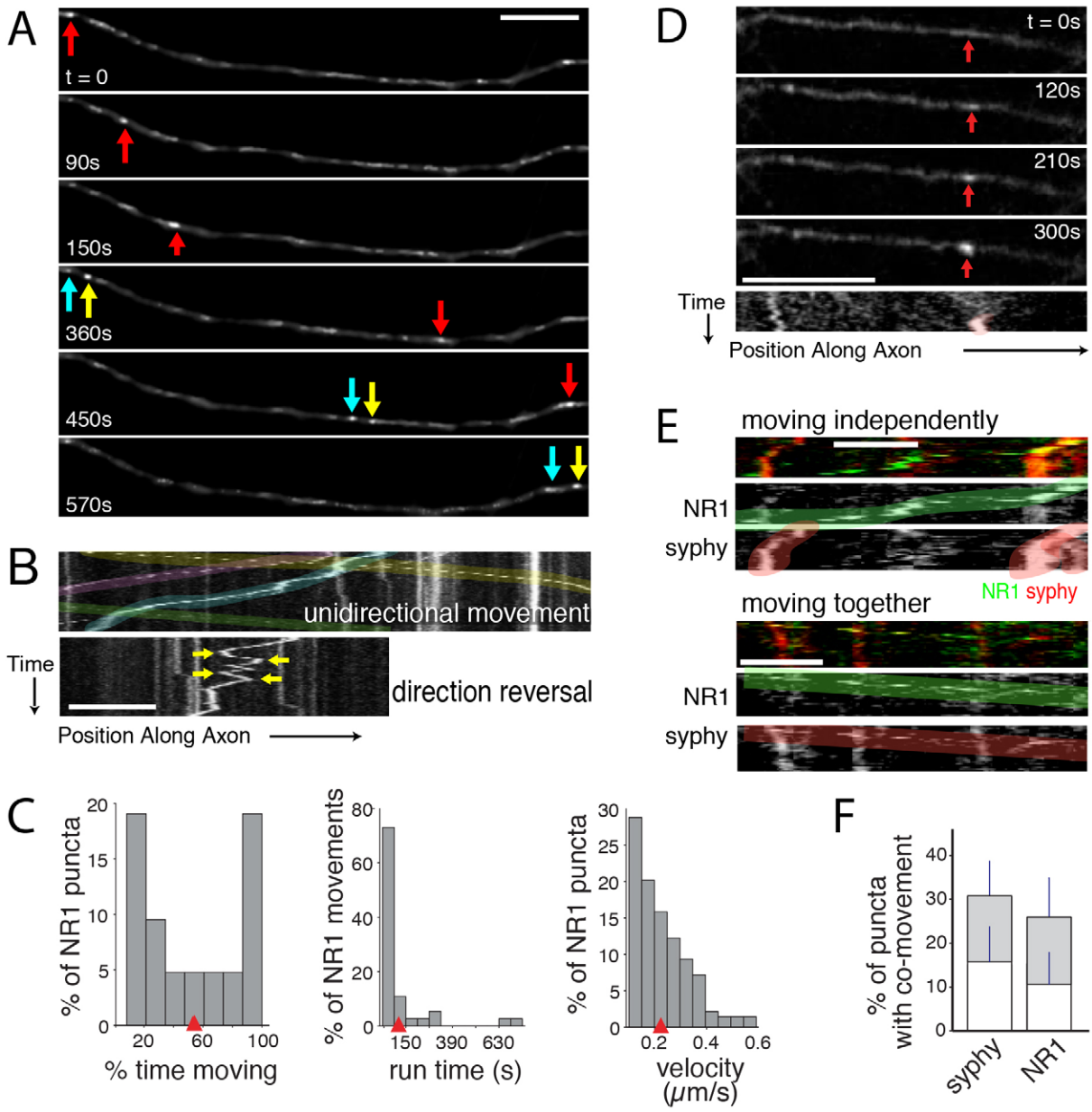

Fig. 5. NR1 is delivered to presynaptic terminals in mobile transport packets distinct from synaptic vesicle precursors. (A) Time-lapse images of NR1–GFP puncta. Individual NR1 puncta are tracked with red, yellow or cyan arrows. Most mobile NR1 puncta moved continuously in one direction for extended periods of time. Frames were collected at the indicated times. Scale bar: 10 μm. (B) Kymographs of NR1–GFP movements, demonstrating different types of movement in two different axons. Most NR1 puncta moved linearly in anterograde or retrograde directions (top panel, green, cyan, pink and yellow lines each highlight the movement of an NR1 punctum). Some puncta moved back and forth along the axon (bottom panel, yellow arrows indicate direction changes). On the *y*-axis, one pixel corresponds to 30 s. (C) Histograms of the percentage of time spent moving (left), the duration of continuous movements uninterrupted by pauses (middle), and the instantaneous velocities (right) of NR1–GFP puncta. Red arrowheads indicate the mean (n=21 puncta from 13 axons). Only non-zero values are included. (D) Time-lapse images (first four panels) and kymograph (bottom panel) of spontaneous formation of an NR1–GFP punctum. Individual frames were collected at the indicated times. On the *y*-axis of the kymograph, one pixel corresponds to 30 s. (E) Kymographs of NR1–GFP and synaptophysin–mRFP in the same axons show that NR1 and synaptophysin (syphy) puncta can move either together (bottom set) or independently (top set). Top panels of each set, overlay of NR1–GFP (green) and synaptophysin–mRFP (red). Middle panels of each set, green lines highlight the movements of NR1 puncta. Bottom panels of each set, pink lines highlight the movements of synaptophysin puncta. NR1 and synaptophysin can move together over either short or long distances, but are more often observed moving independently. On the *y*-axis, one pixel corresponds to 30 s. Scale bars: 5 μm. (F) Plot of the percentage of synaptophysin puncta per axon that moved with NR1 (syphy) and the percentage of NR1 puncta that moved with synaptophysin (NR1) at some point during imaging (n=53 NR1 puncta and 45 synaptophysin puncta in seven axons). Values in the plot are means±s.e.m.. Gray, puncta that moved together part of the time. White, mobile puncta that appeared together throughout imaging.

necessary to define the prevalence, localization and dynamics of axonal and presynaptic NMDARs. Here, we used fluorescence live confocal imaging combined with immunoisolation from synaptosomes and ultrasynaptic fractionation to show for the first time that NMDARs are present in the active zones and synaptic vesicles of presynaptic terminals in developing cortical neurons

Journal of Cell Science (2015) 128, 768–780 doi:10.1242/jcs.162362

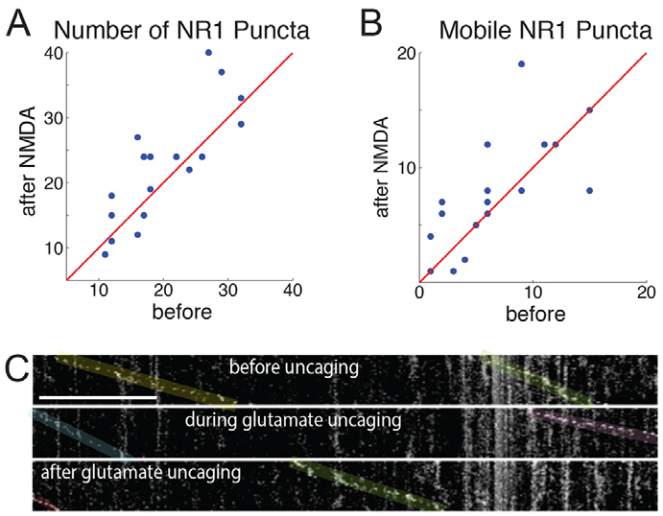

Fig. 6. The distribution and mobility of axonal NMDARs is insensitive to acute changes in activity. (A,B) Plots of the effects of acute exposure to NMDA on the total number of NR1 puncta (A) and the number of mobile NR1 puncta (B) within segments of axons. Each point corresponds to the number of puncta before and after treatment for the same axon. Points above the red line represent an increase in the number or mobility after treatment. No significant change was observed with NMDA treatment. Similar results were seen with TTX (data not shown). (C) Local uncaging of glutamate does not alter the appearance or movement of NR1 puncta. Top, before uncaging; middle, during uncaging; bottom, after uncaging. Scale bar: 10 µm.

in vitro and *in vivo*. NMDARs are found at presynaptic terminals from their earliest stages, and their expression within terminals is developmentally regulated.

Spatial distribution and trafficking of axonal NMDARs and comparison to dendritic receptors

Although NMDARs are present as puncta in both axons and dendrites, the morphologies of axonal and dendritic NMDAR puncta are distinct. First, NR1 puncta occur at a lower density in axons than in dendrites [axons, ~0.04 puncta/µm, or 0.1 puncta/µm if hot-spots were also included; dendrites: ~0.3–0.4 puncta/µm at 5–8 DIV (Washbourne et al., 2002)]. Second, we found that axonal NR1 puncta generally appear to be smaller and dimmer than dendritic NR1 puncta in the same neuron. Because axons express a lower density and intensity of NR1 than dendrites, identification of NR1 in the axons would have been difficult without an independent label to initially identify axons (e.g. synaptophysin–mRFP). This might explain why axonal NR1 was missed in previous studies (Bresler et al., 2004; Washbourne et al., 2002).

Trafficking of NMDAR puncta in axons and dendrites was also distinct. In axons, approximately one quarter of the NR1–GFP puncta were mobile, moving at a mean velocity of 0.23 µm/s. In dendrites, a previous study found that a third of dendritic NR1–GFP clusters are mobile, moving at a mean velocity of 0.07 µm/s (Washbourne et al., 2002), although another study failed to detect mobile dendritic NR1–GFP puncta (Bresler et al., 2004). Most NR2A and NR2B clusters are mobile within developing dendrites (Yin et al., 2012; Yin et al., 2011). However, dendritic NR2A and NR2B move anterogradely at ~0.7–0.8 µm/s (Yin et al., 2012; Yin et al., 2011). Similar velocities (~0.7 µm/s) have been reported for KIF17 (Guillaud et al., 2003; Wong-Riley and Besharse, 2012), a motor that transports dendritic NMDARs (Guillaud et al., 2003; Guillaud et al., 2008; Setou et al., 2000; Song et al., 2009; Yin et al., 2012; Yin et al., 2011).

It is unclear which anterograde motors transport axonal NMDARs. NR2 subunits target NR1 to postsynaptic membranes (Barria and Malinow, 2002). In dendrites, NR2B-containing NMDARs are transported by KIF17 (Guillaud et al., 2003; Guillaud et al., 2008; Setou et al., 2000; Yin et al., 2012; Yin et al., 2011). KIF17 does not enter axons (Guillaud et al., 2003; Song et al., 2009), suggesting that KIF17 is not responsible for NMDAR transport in axons. Because it is likely that NMDARs are transported by distinct motors in axons and dendrites, identification of the responsible motors in future experiments could allow us to selectively reduce expression of either presynaptic or postsynaptic NMDARs in order to understand their distinct functions.

Dynamic NMDARs in axonal growth cones

We also observed dynamic NR1 in nascent axonal growth cones. Surprisingly, NR1 often appeared at sites of growth cone induction even before growth cones appeared. NR1 might be a component of vesicles that supply membrane for growth. Alternatively, NMDARs might regulate growth cone formation or behavior. Consistent with the latter hypothesis, growth cone behavior is strongly regulated by neurotransmitters and intracellular Ca^{2+} (Gomez and Spitzer, 2000; Henley et al., 2004; Ruediger and Bolz, 2007; van Kesteren and Spencer, 2003). In addition to functional NMDARs (Wang et al., 2011), growth cones also express functional AMPARs that are internalized or exposed to the surface upon activity (Schenk et al., 2003). In excitatory neurons, vesicles within axonal growth cones and their filopodia are thought to be capable of glutamate release (Sabo and McAllister, 2003), raising the intriguing possibility that both NMDA and AMPA receptors in growth cones might act as autoreceptors.

Presynaptic NMDARs

Elegant work has provided evidence that NMDARs regulate presynaptic plasticity in the visual and somatosensory neocortex, entorhinal cortex, hippocampus, amygdala, cerebellum and spinal cord (Bardoni et al., 2004; Bender et al., 2006; Berretta and Jones, 1996; Brasier and Feldman, 2008; Buchanan et al., 2012; Casado et al., 2000; Casado et al., 2002; Corlew et al., 2007; Duguid and Smart, 2004; Fiszman et al., 2005; Glitsch and Marty, 1999; Humeau et al., 2003; Jourdain et al., 2007; Li and Han, 2007; Li et al., 2008; Liu et al., 1997; Mameli et al., 2005; Rodríguez-Moreno et al., 2011; Rodríguez-Moreno and Paulsen, 2008; Sjöström et al., 2003; Yang et al., 2006). At least in certain developing neurons, the responsible receptors are found in the presynaptic rather than in the postsynaptic neuron. Recently, several studies have provided convincing functional evidence that the relevant receptors are localized to axons (Buchanan et al., 2012; McGuinness et al., 2010; Rodríguez-Moreno et al., 2011). However, it remained unclear whether these receptors were distributed throughout the axon, concentrated at presynaptic terminals or located in microdomains near synapses. Although electron microscopy studies support the existence of presynaptic NMDARs in the cortex and hippocampus, these studies have not been definitive because there is inconsistency in whether they are found at excitatory presynaptic terminals, in the timing and abundance of their expression, and in their precise localization within terminals (Aoki et al., 2003; Charton et al., 1999; Corlew et al., 2007; DeBiasi et al., 1996; Fujisawa and Aoki, 2003;

Journal of Cell Science (2015) 128, 768–780 doi:10.1242/jcs.162362

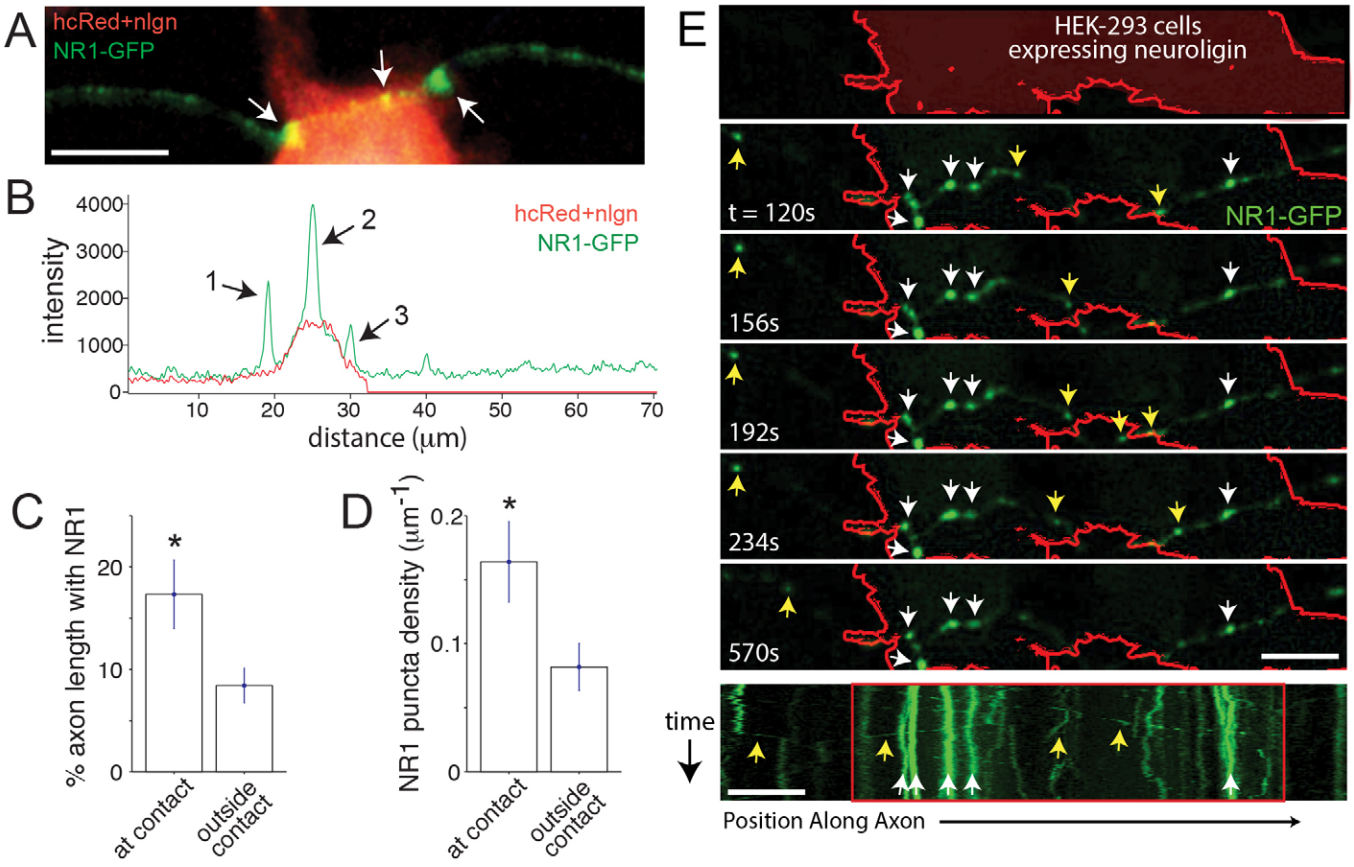

Fig. 7. Trans-synaptic signaling through neuroligin is sufficient to induce stable accumulation of NR1 at developing presynaptic terminals. (A) Fluorescence image showing NR1 (green) accumulation (arrows) at contacts with a neuroligin-expressing HEK-293 cell (red). (B) Line-intensity plot of relative intensity of NR1 and hcRed+neuroligin (nlgn) over distance for another example of hemi-synaptic contact. Pronounced NR1 puncta occurred at three sites within contact with the neuroligin expressing HEK-293 cell (arrows). (C,D) The density of NR1 puncta (D) and the percentage of the axon length containing NR1 puncta (C) were both increased in regions of axon that were contacted by neuroligin-expressing HEK-293 cells when compared to neighboring regions of the same axons. Data are mean±s.e.m. (n=12 contacts). (E) Time-lapse images of NR1–GFP (green) in an axon in contact with neuroligin-expressing HEK-293 cells (red in top panel, red outline in time-lapse). Bottom panel, kymograph of NR1 movements in the same region of the axon. Several large, bright puncta were present and stable at the site of contact with neuroligin (white arrows). In the non-contact regions of the axon, NR1 puncta remained mobile. Multiple small, mobile NR1 puncta also moved through the contact region (yellow arrows). Scale bars: 10 μm.

Jourdain et al., 2007; McGuinness et al., 2010; Siegel et al., 1994).

Here, we have shown that NR1, the obligate subunit of NMDARs, is clustered at presynaptic terminals *in vitro* and *in vivo*. This clustering occurs early in synapse development. Surprisingly, presynaptic NMDARs could be found in synaptic vesicles of both excitatory and inhibitory synapses. The presence of NR1 in association with synaptic vesicles suggests that, in analogy to presynaptic AMPARs, NMDARs can be dynamically internalized by endocytosis and exposed to the presynaptic membrane by exocytosis in response to electrical activity and activation of signal transduction cascades. In addition, the localization of presynaptic NMDARs is developmentally regulated given that NMDARs are not found in synaptic vesicles in mature neurons *in vivo*, consistent with previous studies of presynaptic NMDAR function in cortical slices (Corlew et al., 2007; Wang et al., 2011).

It has recently been shown that NMDARs regulate presynaptic development (Sceniak et al., 2012). Future experiments will be necessary to determine whether presynaptic NMDARs are responsible for this NMDAR-dependent regulation; however, the early appearance of NMDARs at presynaptic terminals is consistent with a role for presynaptic NMDARs. This hypothesis is compelling given the prevalence of postsynaptically silent synapses during circuit development (Groc et al., 2006; Isaac, 2003). How might presynaptic NMDARs regulate presynaptic terminal development? One possibility is that NMDARs regulate presynaptic development by locally increasing Ca^{2+} influx. Ca^{2+} influx regulates the transport of synaptic vesicle proteins along axons during synaptogenesis and increases the anchoring of synaptic vesicle precursors at sites of synapse formation (Sabo et al., 2006), but the source of this Ca^{2+} signal has not been identified.

Here, we demonstrated that NR1 is recruited to sites of presynaptic terminal formation by trans-synaptic adhesion through postsynaptic neuroligin. Given that neuroligin exerts its synapse-organizing effects through its interaction with neurexin on the presynaptic side (Dean et al., 2003; Ichtchenko et al., 1995; Levinson et al., 2005; Nguyen and Südhof, 1997; Scheiffele et al., 2000; Varoqueaux et al., 2006), a link must exist between neurexin adhesion (or clustering) and recruitment of NMDARs to presynaptic terminals. In dendrites, transport of NR2B-containing NMDARs occurs through an interaction with a scaffolding complex that contains MALS/Velis/mLin7, CASK/mLin2 and

Journal of Cell Science (2015) 128, 768–780 doi:10.1242/jcs.162362

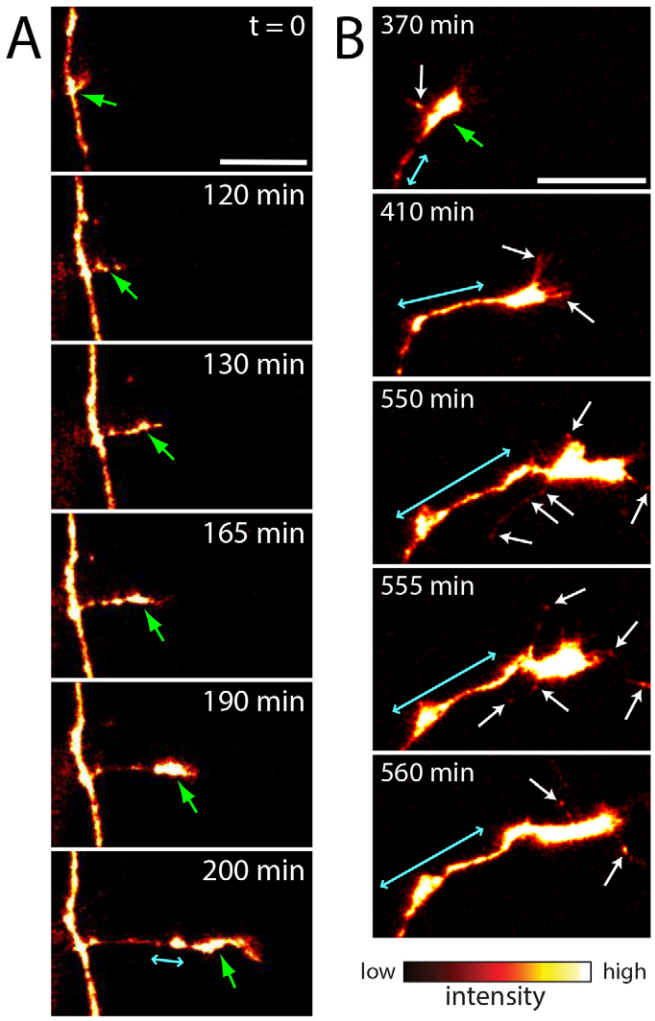

Fig. 8. NR1 is dynamic within axonal growth cones, including new, extending and retracting growth cones. (A,B) Time-lapse images of NR1–GFP in a newly formed axonal growth cone. The same growth cone is shown in A and B, but the images in B were taken after the growth cone had advanced more than 100 μm from the original axon shaft. Fluorescence is pseudocolored according to the indicated intensity scale to enhance visualization of small puncta in the filopodia. Bright NR1 puncta are present in the axonal growth cone (green arrows) and the regions of axon immediately adjacent to the growth cone (cyan lines), including a persistent, large, bright swelling a short distance from the growth cone. NR1 is present in the newly formed growth cone (A), and NR1 fluorescence is elevated in the axon shaft prior to emergence of the growth cone (t=0). NR1 remains present in the growth cone as it advances (B), and its fluorescence within the growth cone and the proximal axon is highly dynamic. NR1 puncta also rapidly enter and leave the growth cone periphery, including filopodia (white arrows). The pattern and dynamics of NR1 within this growth cone are representative of 15 growth cones imaged. Scale bars: 10 μm.

Mint1/X11/mLin10 (Setou et al., 2000). Neurexin can also interact with CASK (Butz et al., 1998; Hata et al., 1996; Mukherjee et al., 2008; Zhang et al., 2001), providing a possible mechanism to link NMDARs to neurexin. This could represent a general mechanism for accumulation of NMDARs at presynaptic terminals because several additional trans-synaptic adhesion proteins, including SynCAMs and APP, can also interact with this complex (Bury and Sabo, 2010).

Our results demonstrate that presynaptic NMDARs are in the right place at the right time to regulate presynaptic development. Previous studies have shown that axonal NMDARs acutely regulate presynaptic transmitter release during postnatal development (Corlew et al., 2008; Pinheiro and Mulle, 2008). Taken together, these data support a new model of postnatal synapse development in which NMDARs occupy a privileged position within presynaptic active zones, where they ultimately act as auto-receptors to promote the development and plasticity of individual presynaptic boutons. They also suggest that prolonged disruption of trafficking, localization or function of presynaptic NMDARs is likely to result in abnormal synapse development. Consistent with this, presynaptic NMDARs have been suggested to play roles in epilepsy (Yang et al., 2007; Yang et al., 2006) and fetal alcohol spectrum disorders (Valenzuela et al., 2008). Mutations in NMDAR subunits are associated with autism, intellectual disability and epilepsy (Endele et al., 2010; Hamdan et al., 2011; O'Roak et al., 2011; O'Roak et al., 2012a; O'Roak et al., 2012b; Tarabeux et al., 2010; Yoo et al., 2012), and it will be interesting to determine whether presynaptic NMDARs are affected by these mutations and how presynaptic NMDARs might contribute to pathogenesis of these diseases.

MATERIALS AND METHODS

Neuronal cultures and transfection

Neurons were dissociated from visual cortices of 0–3-day-old Sprague-Dawley rats, cultured on glial monolayers and transfected, essentially as previously described (Berry et al., 2012; Bury and Sabo, 2011; Bury and Sabo, 2014; Sceniak et al., 2012). For most experiments, neurons were plated on a monolayer of cortical astrocytes in Neurobasal-A medium with glutamax and B27 supplement (Invitrogen). For NR1 immunofluorescence, neurons were plated directly on poly-L-lysine-coated coverslips, in the absence of glia (because glia can express NR1). Astrocytes were grown on collagen (BD Biosciences) and poly-D-lysine (Sigma)-coated coverslips in minimum essential medium (Invitrogen) with glutamax, 10% fetal calf serum (Sigma), glucose (Sigma), N2 supplement (Invitrogen), and penicillin-streptomycin. At 2–4 DIV, neuron cultures were treated with anti-mitotic (5′fluoro-2′dioxy-uridine/uridine; Sigma). Neurons were transfected with NR1–GFP and synaptophysin–mRFP, synaptophysin–mCherry or pTagRFP at 5–10 DIV using Lipofectamine 2000 (Invitrogen). In some experiments, neurons were transfected with synaptophysin-GFP and immunolabled for NR1. All animal experiments were conducted with an approved protocol from the Case Western Reserve University Institutional Animal Care and Use Committee, in compliance with the National Institutes of Health guidelines for the care and use of experimental animals.

Presynaptic terminal induction assay

HEK-293 cells were maintained in Dulbecco's modified Eagle's medium (DMEM) containing 10% fetal calf serum and penicillin-streptomycin. For presynaptic terminal induction, HEK-293 cells were transfected with HA–neuroligin-1 and hcRed or dsRed. At 20–30 h after transfection, cells were dissociated, washed and added to neurons (6–12 DIV). After 24–48 h, cells were fixed and immunolabeled or imaged live.

Immunocytochemistry

With the exception of NR1 labeling, cells were fixed with 4% paraformaldehyde in 0.1 M phosphate-buffered saline (PBS) containing 4% sucrose and permeabilized with 0.2% Triton X-100 in PBS. For NR1, neurons were fixed with −20℃ methanol for 10 min then permeabilized with 0.025% Triton X-100 for 2 min. Primary antibodies were chicken anti-MAP2 (Thermo Scientific), anti-tau-1 (Synaptic Systems), rabbit anti-GFP (Invitrogen) and mouse anti-NR1 (BD Biosciences) antibodies. Secondary antibodies were an anti-chicken-IgG antibody conjugated to Alexa Fluor 647 and anti-mouse- or rabbit-IgG antibody conjugated to Alexa Fluor 555 or 488.

Imaging

Imaging was performed on a Nikon C1 Plus confocal system on a Nikon Ti-E inverted microscope with 488 nm Ar, 543 nm HeNe and 633 nm

HeNe lasers and 40× 1.0 NA and 0.95 NA objectives. For immunocytochemistry, 3D image stacks were collected using EasyC1 software (Nikon) with 2×Kalman averaging, a pixel size of 90–115 nm and 16-bit pixel depth. Each channel was imaged separately to avoid bleed-through. Imaging parameters were optimized to maintain fluorescence within the linear range and maximize intensity resolution. For live imaging, neurons were imaged with continual perfusion with artificial cerebrospinal fluid (ACSF, in mM: 120 NaCl, 3 KCl, 2 $CaCl_2$, 2 $MgCl_2$, 30 D-glucose, 20 HEPES, and 0.2% sorbitol, pH 7.3) or in culture medium. Imaging in culture medium was performed in a custom-built chamber maintained at 35–37℃. In most live imaging experiments, neurons were fixed after imaging for retrospective immunocytochemistry with MAP2 to confirm axonal identity. For treatment with TTX (1 µM) or NMDA (15–100 µM), imaging was performed in the same axons before and during treatment (beginning 0–10 min after start of treatment). NMDA treatment and glutamate uncaging were performed in the presence of glycine (20 µM) and nominal to low Mg^{2+} (0–0.5 mM). For uncaging, axons were imaged to establish baseline NR1–GFP movement then stimulated by uncaging RuBi-glutamate (30 µM, Tocris) with a 488-nm laser (Fino et al., 2009; Salierno et al., 2010). After stimulation, RuBi-glutamate was removed by washing with ACSF for 2 min, followed by additional imaging. Images were obtained every 1–15 s for 5 min. The effectiveness of glutamate uncaging was confirmed with the Ca^{2+} indicator fluo-4 (Invitrogen).

Ultrastructural fractionation

Synaptosomes were purified from P2 fractions from the pooled cortex of three adult mice (3–6 months old) and of six P12 mice. The tissue was homogenized in 10 ml of ice-cold HB buffer (0.32 M sucrose, 1 mM EDTA, 10 mM Tris-HCl, pH 7.4) containing protease inhibitors, using a glass-Teflon homogenizer. The resultant homogenate was centrifuged at 1000 ***g*** for 5 min at 4℃ in order to remove nuclei and debris, and the supernatant was further centrifuged at 18,900 ***g*** for 10 min at 4℃ to obtain the P2 fraction. The P2 pellet was resuspended in 2 ml of HB buffer and gently stratified on a discontinuous Percoll gradient (3–10%–23%). After a 10 min centrifugation at 18,900 ***g*** at 4℃, the synaptosomal fraction from the 10% and 23% Percoll interface was collected, washed in Krebs buffer (140 mM NaCl, 5 mM KCl, 5 mM NaHCO3, 1.3 mM MgSO4, 1 mM phosphate buffer pH 7.4, 10 mM Tris/Hepes pH 7.4) to eliminate Percoll, and used as the starting material for subsequent ultrafractionation.

Ultrasynaptic fractionation was performed according to Feligioni et al. (Feligioni et al., 2006). Synaptosomes were pelleted by centrifugation (16,000 ***g***, 5 min, 4℃) and resuspended in 300 µl of 0.32 M sucrose, 0.1 mM $CaCl_2$. An aliquot was removed and kept as 'total'. Synaptosomes were diluted 1:10 in ice-cold 0.1 mM $CaCl_2$ and mixed with an equal volume of 2× solubilization buffer (2% Triton X-100, 40 mM Tris-HCl, pH 6, 4℃). After a 30-min incubation at 4℃, the insoluble material (synaptic junction) was pelleted by centrifugation (40,000 ***g***, 30 min, 4℃). The supernatant (non-synaptic synaptosomal protein; NSSP) was decanted and the proteins precipitated with six volumes of acetone at −20℃ overnight and then centrifuged (18,000 ***g***, 30 min, −15℃). The synaptic junction pellet (containing the insoluble postsynaptic density and the presynaptic active zone) was resuspended in ten volumes of 1× solubilization buffer (1% Triton X-100, 20 mM Tris-HCl, pH 8, 4℃), incubated for 30 min at 4℃ then centrifuged (40,000 ***g***, 30 min, 4℃). The pellet represents the postsynaptic density (PSD). The proteins in the supernatant (presynaptic fraction, AZ) were precipitated in 6 volumes of acetone at −20℃ overnight then centrifuged (18,000×g, 30 min, −15℃). All pellets (NSSP, AZ and PSD) were resuspended in 5% SDS, quantified by a BCA assay and loaded on SDS-PAGE gels for electrophoresis and western blotting. Polyclonal anti-NR2B and monoclonal anti-synaptophysin, anti-PSD95, anti-NR1 antibodies were from Synaptic Systems. The monoclonal anti-panSHANK antibody was from the UC Davis/NIH NeuroMab Facility; the anti-NR2A antibody was from BD Biosciences. Exposures were optimized in order to avoid saturation of the signal in any of the lanes (P12 and adult were performed in the same western blot and quantified at the same exposures for a given experiment to allow comparison across age for a given antibody). Protease inhibitors were used in all purification steps.

Synaptic vesicle immunoisolation

Eupergit C1Z methacrylate microbeads (1 µm diameter; Röhm Pharmaceuticals, Darmstadt, Germany) were blocked with glycine or conjugated with affinity-purified goat anti-rabbit-IgG antibodies (IgG; Sigma) as previously described (Burger et al., 1991; Fattorini et al., 2009). Affinity-purified anti-VGLUT1, -VGLUT2 and -VGAT antibodies (Synaptic Systems) were conjugated with the covalently bound secondary antibodies, generating IgG-coated anti-VGLUT1, anti-VGLUT2 or anti-VGAT beads. Beads coated with glycine or secondary antibodies only were used as negative controls (mock beads). Aliquots of the LS1 fraction (300 µg protein; Huttner et al., 1983) obtained from osmotic lysis of cortical synaptosomes prepared from either adult (3–6 months old) or P6 mice were incubated for 2–4 h at 4℃ in phosphate-buffered saline (PBS) with bead preparations (50–70 µl settled beads in 500 µl final volume) under constant rotation. After centrifugation at 1000 ***g*** for 1 min and repeated washes in PBS, corresponding amounts of bead pellets and supernatant fractions were subjected to SDS-PAGE on 10% polyacrylamide gels. Gels were electrophoretically transferred to nitrocellulose membranes and immunoblotted with polyclonal anti-synaptophysin or monoclonal anti-NR1 antibodies. Quantification of the recovered immunoreactivity was performed by densitometric analysis of the fluorograms and by data interpolation into a standard curve of mouse brain LS1 fraction run in parallel. Amounts of synaptophysin and NR1 associated with immunoisolated vesicles were expressed as a percentage of the total input of LS1 fraction added to the samples. Experiments were repeated at least three times. Membranes were also probed with affinity-purified anti-VGLUT1, -VGLUT2 and -VGAT antibodies to confirm the immunoisolation of glutamatergic and GABAergic synaptic vesicles.

Subcellular fractionation

Subcellular fractions were prepared from 5–6-week-old male Sprague-Dawley rat forebrain, and synaptic vesicles were purified through controlled-pore glass chromatography (Huttner et al., 1983). Purified synaptic vesicles (USV) were recovered by high-speed centrifugation and resuspended in 0.3 M glycine, 5 mM Hepes (pH 7.4) at a protein concentration of 1 mg/ml.

Imaging data analysis

Custom macros in ImageJ (NIH, Bethesda, MD) were used to conduct automated image analysis. Maximum intensity *z*-projections were made then filtered using a Gaussian blur. Intensities were measured along axon lengths to generate line profiles. Measurements were transferred to Matlab (Mathworks, Natick, MA) for quantification using custom-written functions. A threshold of 1–2 standard deviations above the mean intensity was used to define an NR1 punctum or hot-spot. For experiments involving axon–HEK-293 cell contact, puncta distributions were compared within and outside contact regions. A MAP2 signal that was 2.5 standard deviations above the mean intensity was used to blindly identify presynaptic contact with dendrites. For colocalization and cross-correlation, each channel was analyzed independently while blind to all other channels.

For live imaging, NR1 movements were tracked in ImageJ then further analyzed in Matlab. Axons were included if at least one punctum moved within the field of view. Movements were defined as instantaneous velocities >0.1 µm/s. Run times correspond to the length of time that instantaneous velocities were continuously >0.1 µm/s. Because some runs began before or continued after the imaging period, long runs may be truncated and under-represented.

Competing interests

The authors declare no competing or financial interests.

Author contributions

I.G., S.D., S.G., K.N.F., L.A.D.B., F. Bosco and S.L.S. performed experiments and analyzed data. S.G., F. Benfenati and S.L.S. designed experiments. I.G., S.D., S.G., K.N.F., M.P.S., F. Benfenati and S.L.S. wrote the manuscript.

Funding

The work was funded by by grants from the National Institutes of Health [grant number R01MH096908 to S.L.S.]; and the Ministero dell'Istruzione, dell'

Università e della Ricerca (MIUR) [grants PRIN to F.B.; FIRB 2010 'Futuro in ricerca' to S.G.]. Deposited in PMC for release after 12 months.

Supplementary material

Supplementary material available online at
http://jcs.biologists.org/lookup/suppl/doi:10.1242/jcs.162362/-/DC1

References

Aoki, C., Fujisawa, S., Mahadomrongkul, V., Shah, P. J., Nader, K. and Erisir, A. (2003). NMDA receptor blockade in intact adult cortex increases trafficking of NR2A subunits into spines, postsynaptic densities, and axon terminals. *Brain Res.* **963**, 139-149.

Bardoni, R., Torsney, C., Tong, C. K., Prandini, M. and MacDermott, A. B. (2004). Presynaptic NMDA receptors modulate glutamate release from primary sensory neurons in rat spinal cord dorsal horn. *J. Neurosci.* **24**, 2774-2781.

Barria, A. and Malinow, R. (2002). Subunit-specific NMDA receptor trafficking to synapses. *Neuron* **35**, 345-353.

Bender, V. A., Bender, K. J., Brasier, D. J. and Feldman, D. E. (2006). Two coincidence detectors for spike timing-dependent plasticity in somatosensory cortex. *J. Neurosci.* **26**, 4166-4177.

Bernhardt, R. and Matus, A. (1984). Light and electron microscopic studies of the distribution of microtubule-associated protein 2 in rat brain: a difference between dendritic and axonal cytoskeletons. *J. Comp. Neurol.* **226**, 203-221.

Berretta, N. and Jones, R. S. (1996). Tonic facilitation of glutamate release by presynaptic N-methyl-D-aspartate autoreceptors in the entorhinal cortex. *Neuroscience* **75**, 339-344.

Berry, C. T., Sceniak, M. P., Zhou, L. and Sabo, S. L. (2012). Developmental up-regulation of vesicular glutamate transporter-1 promotes neocortical presynaptic terminal development. *PLoS ONE* **7**, e50911.

Binder, L. I., Frankfurter, A. and Rebhun, L. I. (1985). The distribution of tau in the mammalian central nervous system. *J. Cell Biol.* **101**, 1371-1378.

Brasier, D. J. and Feldman, D. E. (2008). Synapse-specific expression of functional presynaptic NMDA receptors in rat somatosensory cortex. *J. Neurosci.* **28**, 2199-2211.

Bresler, T., Shapira, M., Boeckers, T., Dresbach, T., Futter, M., Garner, C. C., Rosenblum, K., Gundelfinger, E. D. and Ziv, N. E. (2004). Postsynaptic density assembly is fundamentally different from presynaptic active zone assembly. *J. Neurosci.* **24**, 1507-1520.

Buchanan, K. A., Blackman, A. V., Moreau, A. W., Elgar, D., Costa, R. P., Lalanne, T., Tudor Jones, A. A., Oyrer, J. and Sjöström, P. J. (2012). Target-specific expression of presynaptic NMDA receptors in neocortical microcircuits. *Neuron* **75**, 451-466.

Burger, P. M., Hell, J., Mehl, E., Krasel, C., Lottspeich, F. and Jahn, R. (1991). GABA and glycine in synaptic vesicles: storage and transport characteristics. *Neuron* **7**, 287-293.

Bury, L. A. and Sabo, S. L. (2010). How it's made: the synapse. *Mol. Interv.* **10**, 282-292.

Bury, L. A. and Sabo, S. L. (2011). Coordinated trafficking of synaptic vesicle and active zone proteins prior to synapse formation. *Neural Dev.* **6**, 24.

Bury, L. A. and Sabo, S. L. (2014). Dynamic mechanisms of neuroligin-dependent presynaptic terminal assembly in living cortical neurons. *Neural Dev.* **9**, 13.

Butz, S., Okamoto, M. and Südhof, T. C. (1998). A tripartite protein complex with the potential to couple synaptic vesicle exocytosis to cell adhesion in brain. *Cell* **94**, 773-782.

Casado, M., Dieudonné, S. and Ascher, P. (2000). Presynaptic N-methyl-D-aspartate receptors at the parallel fiber-Purkinje cell synapse. *Proc. Natl. Acad. Sci. USA* **97**, 11593-11597.

Casado, M., Isope, P. and Ascher, P. (2002). Involvement of presynaptic N-methyl-D-aspartate receptors in cerebellar long-term depression. *Neuron* **33**, 123-130.

Charton, J. P., Herkert, M., Becker, C. M. and Schröder, H. (1999). Cellular and subcellular localization of the 2B-subunit of the NMDA receptor in the adult rat telencephalon. *Brain Res.* **816**, 609-617.

Christie, J. M. and Jahr, C. E. (2008). Dendritic NMDA receptors activate axonal calcium channels. *Neuron* **60**, 298-307.

Christie, J. M. and Jahr, C. E. (2009). Selective expression of ligand-gated ion channels in L5 pyramidal cell axons. *J. Neurosci.* **29**, 11441-11450.

Corlew, R., Wang, Y., Ghermazien, H., Erisir, A. and Philpot, B. D. (2007). Developmental switch in the contribution of presynaptic and postsynaptic NMDA receptors to long-term depression. *J. Neurosci.* **27**, 9835-9845.

Corlew, R., Brasier, D. J., Feldman, D. E. and Philpot, B. D. (2008). Presynaptic NMDA receptors: newly appreciated roles in cortical synaptic function and plasticity. *Neuroscientist* **14**, 609-625.

Dean, C., Scholl, F. G., Choih, J., DeMaria, S., Berger, J., Isacoff, E. and Scheiffele, P. (2003). Neurexin mediates the assembly of presynaptic terminals. *Nat. Neurosci.* **6**, 708-716.

DeBiasi, S., Minelli, A., Melone, M. and Conti, F. (1996). Presynaptic NMDA receptors in the neocortex are both auto- and heteroreceptors. *Neuroreport* **7**, 2773-2776.

Duguid, I. C. and Smart, T. G. (2004). Retrograde activation of presynaptic NMDA receptors enhances GABA release at cerebellar interneuron-Purkinje cell synapses. *Nat. Neurosci.* **7**, 525-533.

Ehlers, M. D., Fung, E. T., O'Brien, R. J. and Huganir, R. L. (1998). Splice variant-specific interaction of the NMDA receptor subunit NR1 with neuronal intermediate filaments. *J. Neurosci.* **18**, 720-730.

Endele, S., Rosenberger, G., Geider, K., Popp, B., Tamer, C., Stefanova, I., Milh, M., Kortüm, F., Fritsch, A., Pientka, F. K. et al. (2010). Mutations in GRIN2A and GRIN2B encoding regulatory subunits of NMDA receptors cause variable neurodevelopmental phenotypes. *Nat. Genet.* **42**, 1021-1026.

Fattorini, G., Verderio, C., Melone, M., Giovedì, S., Benfenati, F., Matteoli, M. and Conti, F. (2009). VGLUT1 and VGAT are sorted to the same population of synaptic vesicles in subsets of cortical axon terminals. *J. Neurochem.* **110**, 1538-1546.

Feligioni, M., Holman, D., Haglerod, C., Davanger, S. and Henley, J. M. (2006). Ultrastructural localisation and differential agonist-induced regulation of AMPA and kainate receptors present at the presynaptic active zone and postsynaptic density. *J. Neurochem.* **99**, 549-560.

Fino, E., Araya, R., Peterka, D. S., Salierno, M., Etchenique, R. and Yuste, R. (2009). RuBi-glutamate: two-photon and visible-light photoactivation of neurons and dendritic spines. *Front. Neural Circuits* **3**, 2.

Fiszman, M. L., Barberis, A., Lu, C., Fu, Z., Erdélyi, F., Szabó, G. and Vicini, S. (2005). NMDA receptors increase the size of GABAergic terminals and enhance GABA release. *J. Neurosci.* **25**, 2024-2031.

Fujisawa, S. and Aoki, C. (2003). In vivo blockade of N-methyl-D-aspartate receptors induces rapid trafficking of NR2B subunits away from synapses and out of spines and terminals in adult cortex. *Neuroscience* **121**, 51-63.

Glitsch, M. and Marty, A. (1999). Presynaptic effects of NMDA in cerebellar Purkinje cells and interneurons. *J. Neurosci.* **19**, 511-519.

Gomez, T. M. and Spitzer, N. C. (2000). Regulation of growth cone behavior by calcium: new dynamics to earlier perspectives. *J. Neurobiol.* **44**, 174-183.

Granger, A. J., Gray, J. A., Lu, W. and Nicoll, R. A. (2011). Genetic analysis of neuronal ionotropic glutamate receptor subunits. *J. Physiol.* **589**, 4095-4101.

Groc, L., Gustafsson, B. and Hanse, E. (2006). AMPA signalling in nascent glutamatergic synapses: there and not there! *Trends Neurosci.* **29**, 132-139.

Grosshans, D. R., Clayton, D. A., Coultrap, S. J. and Browning, M. D. (2002). LTP leads to rapid surface expression of NMDA but not AMPA receptors in adult rat CA1. *Nat. Neurosci.* **5**, 27-33.

Guillaud, L., Setou, M. and Hirokawa, N. (2003). KIF17 dynamics and regulation of NR2B trafficking in hippocampal neurons. *J. Neurosci.* **23**, 131-140.

Guillaud, L., Wong, R. and Hirokawa, N. (2008). Disruption of KIF17-Mint1 interaction by CaMKII-dependent phosphorylation: a molecular model of kinesin-cargo release. *Nat. Cell Biol.* **10**, 19-29.

Hamdan, F. F., Gauthier, J., Araki, Y., Lin, D. T., Yoshizawa, Y., Higashi, K., Park, A. R., Spiegelman, D., Dobrzeniecka, S., Piton, A. et al.; S2D Group (2011). Excess of de novo deleterious mutations in genes associated with glutamatergic systems in nonsyndromic intellectual disability. *Am. J. Hum. Genet.* **88**, 306-316.

Hata, Y., Butz, S. and Südhof, T. C. (1996). CASK: a novel dlg/PSD95 homolog with an N-terminal calmodulin-dependent protein kinase domain identified by interaction with neurexins. *J. Neurosci.* **16**, 2488-2494.

Henley, J. R., Huang, K. H., Wang, D. and Poo, M. M. (2004). Calcium mediates bidirectional growth cone turning induced by myelin-associated glycoprotein. *Neuron* **44**, 909-916.

Herkert, M., Röttger, S. and Becker, C. M. (1998). The NMDA receptor subunit NR2B of neonatal rat brain: complex formation and enrichment in axonal growth cones. *Eur. J. Neurosci.* **10**, 1553-1562.

Heynen, A. J., Quinlan, E. M., Bae, D. C. and Bear, M. F. (2000). Bidirectional, activity-dependent regulation of glutamate receptors in the adult hippocampus in vivo. *Neuron* **28**, 527-536.

Humeau, Y., Shaban, H., Bissière, S. and Lüthi, A. (2003). Presynaptic induction of heterosynaptic associative plasticity in the mammalian brain. *Nature* **426**, 841-845.

Huttner, W. B., Schiebler, W., Greengard, P. and De Camilli, P. (1983). Synapsin I (protein I), a nerve terminal-specific phosphoprotein. III. Its association with synaptic vesicles studied in a highly purified synaptic vesicle preparation. *J. Cell Biol.* **96**, 1374-1388.

Ichtchenko, K., Hata, Y., Nguyen, T., Ullrich, B., Missler, M., Moomaw, C. and Südhof, T. C. (1995). Neuroligin 1: a splice site-specific ligand for beta-neurexins. *Cell* **81**, 435-443.

Isaac, J. T. (2003). Postsynaptic silent synapses: evidence and mechanisms. *Neuropharmacology* **45**, 450-460.

Jourdain, P., Bergersen, L. H., Bhaukaurally, K., Bezzi, P., Santello, M., Domercq, M., Matute, C., Tonello, F., Gundersen, V. and Volterra, A. (2007). Glutamate exocytosis from astrocytes controls synaptic strength. *Nat. Neurosci.* **10**, 331-339.

Kosik, K. S. and Finch, E. A. (1987). MAP2 and tau segregate into dendritic and axonal domains after the elaboration of morphologically distinct neurites: an immunocytochemical study of cultured rat cerebrum. *J. Neurosci.* **7**, 3142-3153.

Lee, H., Dean, C. and Isacoff, E. (2010). Alternative splicing of neuroligin regulates the rate of presynaptic differentiation. *J. Neurosci.* **30**, 11435-11446.

Levinson, J. N., Chéry, N., Huang, K., Wong, T. P., Gerrow, K., Kang, R., Prange, O., Wang, Y. T. and El-Husseini, A. (2005). Neuroligins mediate excitatory and inhibitory synapse formation: involvement of PSD-95 and neurexin-1beta in neuroligin-induced synaptic specificity. *J. Biol. Chem.* **280**, 17312-17319.

Li, Y. H. and Han, T. Z. (2007). Glycine binding sites of presynaptic NMDA receptors may tonically regulate glutamate release in the rat visual cortex. *J. Neurophysiol.* **97**, 817-823.
Li, Y. H., Han, T. Z. and Meng, K. (2008). Tonic facilitation of glutamate release by glycine binding sites on presynaptic NR2B-containing NMDA autoreceptors in the rat visual cortex. *Neurosci. Lett.* **432**, 212-216.
Liu, H., Mantyh, P. W. and Basbaum, A. I. (1997). NMDA-receptor regulation of substance P release from primary afferent nociceptors. *Nature* **386**, 721-724.
Luo, J. H., Fu, Z. Y., Losi, G., Kim, B. G., Prybylowski, K., Vissel, B. and Vicini, S. (2002). Functional expression of distinct NMDA channel subunits tagged with green fluorescent protein in hippocampal neurons in culture. *Neuropharmacology* **42**, 306-318.
Madara, J. C. and Levine, E. S. (2008). Presynaptic and postsynaptic NMDA receptors mediate distinct effects of brain-derived neurotrophic factor on synaptic transmission. *J Neurophysiol.* **100**, 3175-3184.
Mameli, M., Carta, M., Partridge, L. D. and Valenzuela, C. F. (2005). Neurosteroid-induced plasticity of immature synapses via retrograde modulation of presynaptic NMDA receptors. *J. Neurosci.* **25**, 2285-2294.
McGuinness, L., Taylor, C., Taylor, R. D., Yau, C., Langenhan, T., Hart, M. L., Christian, H., Tynan, P. W., Donnelly, P. and Emptage, N. J. (2010). Presynaptic NMDARs in the hippocampus facilitate transmitter release at theta frequency. *Neuron* **68**, 1109-1127.
Mukherjee, K., Sharma, M., Urlaub, H., Bourenkov, G. P., Jahn, R., Südhof, T. C. and Wahl, M. C. (2008). CASK Functions as a Mg2+-independent neurexin kinase. *Cell* **133**, 328-339.
Nguyen, T. and Südhof, T. C. (1997). Binding properties of neuroligin 1 and neurexin 1beta reveal function as heterophilic cell adhesion molecules. *J. Biol. Chem.* **272**, 26032-26039.
O'Roak, B. J., Deriziotis, P., Lee, C., Vives, L., Schwartz, J. J., Girirajan, S., Karakoc, E., Mackenzie, A. P., Ng, S. B., Baker, C. et al. (2011). Exome sequencing in sporadic autism spectrum disorders identifies severe de novo mutations. *Nat. Genet.* **43**, 585-589.
O'Roak, B. J., Vives, L., Fu, W., Egertson, J. D., Stanaway, I. B., Phelps, I. G., Carvill, G., Kumar, A., Lee, C., Ankenman, K. et al. (2012a). Multiplex targeted sequencing identifies recurrently mutated genes in autism spectrum disorders. *Science* **338**, 1619-1622.
O'Roak, B. J., Vives, L., Girirajan, S., Karakoc, E., Krumm, N., Coe, B. P., Levy, R., Ko, A., Lee, C., Smith, J. D. et al. (2012b). Sporadic autism exomes reveal a highly interconnected protein network of de novo mutations. *Nature* **485**, 246-250.
Phillips, G. R., Huang, J. K., Wang, Y., Tanaka, H., Shapiro, L., Zhang, W., Shan, W. S., Arndt, K., Frank, M., Gordon, R. E. et al. (2001). The presynaptic particle web: ultrastructure, composition, dissolution, and reconstitution. *Neuron* **32**, 63-77.
Pinheiro, P. S. and Mulle, C. (2008). Presynaptic glutamate receptors: physiological functions and mechanisms of action. *Nat. Rev. Neurosci.* **9**, 423-436.
Pinheiro, P. S., Rodrigues, R. J., Silva, A. P., Cunha, R. A., Oliveira, C. R. and Malva, J. O. (2003). Solubilization and immunological identification of presynaptic alpha-amino-3-hydroxy-5-methyl-4-isoxazolepropionic acid receptors in the rat hippocampus. *Neurosci. Lett.* **336**, 97-100.
Pinheiro, P. S., Rodrigues, R. J., Rebola, N., Xapelli, S., Oliveira, C. R. and Malva, J. O. (2005). Presynaptic kainate receptors are localized close to release sites in rat hippocampal synapses. *Neurochem. Int.* **47**, 309-316.
Prybylowski, K., Fu, Z., Losi, G., Hawkins, L. M., Luo, J., Chang, K., Wenthold, R. J. and Vicini, S. (2002). Relationship between availability of NMDA receptor subunits and their expression at the synapse. *J. Neurosci.* **22**, 8902-8910.
Rodríguez-Moreno, A. and Paulsen, O. (2008). Spike timing-dependent long-term depression requires presynaptic NMDA receptors. *Nat. Neurosci.* **11**, 744-745.
Rodríguez-Moreno, A., Kohl, M. M., Reeve, J. E., Eaton, T. R., Collins, H. A., Anderson, H. L. and Paulsen, O. (2011). Presynaptic induction and expression of timing-dependent long-term depression demonstrated by compartment-specific photorelease of a use-dependent NMDA receptor antagonist. *J. Neurosci.* **31**, 8564-8569.
Ruediger, T. and Bolz, J. (2007). Neurotransmitters and the development of neuronal circuits. *Adv. Exp. Med. Biol.* **621**, 104-114.
Sabo, S. L. and McAllister, A. K. (2003). Mobility and cycling of synaptic protein-containing vesicles in axonal growth cone filopodia. *Nat. Neurosci.* **6**, 1264-1269.
Sabo, S. L., Gomes, R. A. and McAllister, A. K. (2006). Formation of presynaptic terminals at predefined sites along axons. *J. Neurosci.* **26**, 10813-10825.
Salierno, M., Marceca, E., Peterka, D. S., Yuste, R. and Etchenique, R. (2010). A fast ruthenium polypyridine cage complex photoreleases glutamate with visible or IR light in one and two photon regimes. *J. Inorg. Biochem.* **104**, 418-422.
Sceniak, M. P., Berry, C. T. and Sabo, S. L. (2012). Facilitation of neocortical presynaptic terminal development by NMDA receptor activation. *Neural Dev.* **7**, 8.
Scheiffele, P., Fan, J., Choih, J., Fetter, R. and Serafini, T. (2000). Neuroligin expressed in nonneuronal cells triggers presynaptic development in contacting axons. *Cell* **101**, 657-669.
Schenk, U., Verderio, C., Benfenati, F. and Matteoli, M. (2003). Regulated delivery of AMPA receptor subunits to the presynaptic membrane. *EMBO J.* **22**, 558-568.
Setou, M., Nakagawa, T., Seog, D. H. and Hirokawa, N. (2000). Kinesin superfamily motor protein KIF17 and mLin-10 in NMDA receptor-containing vesicle transport. *Science* **288**, 1796-1802.
Siegel, S. J., Brose, N., Janssen, W. G., Gasic, G. P., Jahn, R., Heinemann, S. F. and Morrison, J. H. (1994). Regional, cellular, and ultrastructural distribution of N-methyl-D-aspartate receptor subunit 1 in monkey hippocampus. *Proc. Natl. Acad. Sci. USA* **91**, 564-568.
Sjöström, P. J., Turrigiano, G. G. and Nelson, S. B. (2003). Neocortical LTD via coincident activation of presynaptic NMDA and cannabinoid receptors. *Neuron* **39**, 641-654.
Song, A. H., Wang, D., Chen, G., Li, Y., Luo, J., Duan, S. and Poo, M. M. (2009). A selective filter for cytoplasmic transport at the axon initial segment. *Cell* **136**, 1148-1160.
Tarabeux, J., Champagne, N., Brustein, E., Hamdan, F. F., Gauthier, J., Lapointe, M., Maios, C., Piton, A., Spiegelman, D., Henrion, E. et al.; Synapse to Disease Team (2010). De novo truncating mutation in Kinesin 17 associated with schizophrenia. *Biol. Psychiatry* **68**, 649-656.
Valenzuela, C. F., Partridge, L. D., Mameli, M. and Meyer, D. A. (2008). Modulation of glutamatergic transmission by sulfated steroids: role in fetal alcohol spectrum disorder. *Brain Res. Rev.* **57**, 506-519.
van Kesteren, R. E. and Spencer, G. E. (2003). The role of neurotransmitters in neurite outgrowth and synapse formation. *Rev. Neurosci.* **14**, 217-231.
Varoqueaux, F., Aramuni, G., Rawson, R. L., Mohrmann, R., Missler, M., Gottmann, K., Zhang, W., Südhof, T. C. and Brose, N. (2006). Neuroligins determine synapse maturation and function. *Neuron* **51**, 741-754.
Wang, P. Y., Petralia, R. S., Wang, Y. X., Wenthold, R. J. and Brenowitz, S. D. (2011). Functional NMDA receptors at axonal growth cones of young hippocampal neurons. *J. Neurosci.* **31**, 9289-9297.
Washbourne, P., Bennett, J. E. and McAllister, A. K. (2002). Rapid recruitment of NMDA receptor transport packets to nascent synapses. *Nat. Neurosci.* **5**, 751-759.
Wong-Riley, M. T. and Besharse, J. C. (2012). The kinesin superfamily protein KIF17: one protein with many functions. *Biomol. Concepts* **3**, 267-282.
Yang, J., Woodhall, G. L. and Jones, R. S. (2006). Tonic facilitation of glutamate release by presynaptic NR2B-containing NMDA receptors is increased in the entorhinal cortex of chronically epileptic rats. *J. Neurosci.* **26**, 406-410.
Yang, J., Wetterstrand, C. and Jones, R. S. (2007). Felbamate but not phenytoin or gabapentin reduces glutamate release by blocking presynaptic NMDA receptors in the entorhinal cortex. *Epilepsy Res.* **77**, 157-164.
Yin, X., Takei, Y., Kido, M. A. and Hirokawa, N. (2011). Molecular motor KIF17 is fundamental for memory and learning via differential support of synaptic NR2A/2B levels. *Neuron* **70**, 310-325.
Yin, X., Feng, X., Takei, Y. and Hirokawa, N. (2012). Regulation of NMDA receptor transport: a KIF17-cargo binding/releasing underlies synaptic plasticity and memory in vivo. *J. Neurosci.* **32**, 5486-5499.
Yoo, H. J., Cho, I. H., Park, M., Yang, S. Y. and Kim, S. A. (2012). Family based association of GRIN2A and GRIN2B with Korean autism spectrum disorders. *Neurosci. Lett.* **512**, 89-93.
Zhang, Y., Luan, Z., Liu, A. and Hu, G. (2001). The scaffolding protein CASK mediates the interaction between rabphilin3a and beta-neurexins. *FEBS Lett.* **497**, 99-102.

Journal of Cell Science